AIMS Mathematics, 11(2): 3703–3723.
DOI: 10.3934/math.2026150
Received: 06 November 2025
Revised: 31 December 2025
Accepted: 22 January 2026
Published: 06 February 2026

https://www.aimspress.com/journal/Math

Research article

Variable convergence rate fuzzy control of chaotic Chua's circuit under impulsive and stochastic disturbances

Yining Zhang[1], Xinran Li[1], Tinglin Zhang[2] and Huasheng Zhang[1,*]

[1] School of Mathematical Sciences, Liaocheng University, Liaocheng Shandong 252059, China
[2] School of Information Engineering, Yancheng Institute of Technology, Yancheng 224051, China

* **Correspondence:** Email: zhanghuasheng@lcu.edu.cn.

Abstract: This paper proposes an intelligent regulation method for dynamically adjusting the convergence rate of nonlinear Chua's circuits subject to impulsive effects and stochastic disturbances, based on a Takagi-Sugeno (T-S) fuzzy model. First, an interval stability criterion for variable convergence rate is established through generalized pole assignment principle, constructing a unified analytical framework that simultaneously incorporates stability margin and dynamic convergence rate indicators. Second, a state feedback fuzzy controller with convergence rate constraints is designed. By constructing a constrained eigenvalue domain, the controller enables active regulation of the system's convergence rate. Furthermore, an intelligent convergence rate regulation algorithm is developed to achieve precise on-demand adjustment for Chua's circuit. Finally, simulation experiments conducted on the original system using the proposed fuzzy controller verify the effectiveness and practical utility of the control strategy.

Keywords: Chua's circuit; stability of variable convergence rate; T-S fuzzy control; impulsive system; stochastic disturbance
Mathematics Subject Classification: 34D20, 93B36, 93C42, 93D09, 93D20

1. Introduction

The Chua's circuit, which comprises an inductor, a resistor, two capacitors, and a Chua's diode [1], can demonstrate diverse nonlinear dynamical phenomena such as bifurcations [2, 3] and chaos [4]. As a fundamental characteristic of complex dynamical systems, chaos has established the nonlinear Chua's circuit as a canonical prototype for chaos research. However, chaotic behavior can lead to unpredictable system dynamics and performance degradation; consequently, control strategies for Chua's circuit have attracted considerable attention [5, 6]. For instance, capacitor synchronization has been a research

focus [7], while pulse stabilization for time-varying Chua's circuit systems under input disturbances has also been investigated [8].

The nonlinearity of the diode in Chua's circuit complicates its analysis. The T-S fuzzy model, first proposed by Takagi and Sugeno in 1985 [9], allows for the application of linear system theory to nonlinear systems [10–12]. This model achieves a global approximation of a nonlinear system by representing its local dynamics as linear subsystems and integrating them through membership functions [13–15]. Modeling Chua's circuit within the T-S fuzzy framework provides a systematic approach for in-depth analysis of its nonlinear dynamics and facilitates control synthesis. For example, a fuzzy pulse control criterion has been proposed for Chua's circuit [16], and a subsequently developed fuzzy sliding mode control scheme has been successfully applied to it [17].

In control theory, an impulse is defined as an instantaneous change of state, typically manifested as a sudden change in signal amplitude [18, 19]. In practice, such impulses are often induced by the instantaneous switching of components or rapid changes in voltage or current in Chua's circuits [20, 21]. Systems subject to such effects, known as impulsive systems, have become a focal research area because they incorporate both continuous and discrete dynamical characteristics [22, 23]. Reference [24] systematically analyzed the impulse effects in Chua's circuit and established stabilization criteria to ensure system stability and controllability. Consequently, the behavioral uncertainty induced by impulses underscores the critical importance of designing effective control strategies for Chua's circuit.

Furthermore, the operation of these systems is inevitably subject to external stochastic noise, which poses significant challenges to control system robustness [25–27]. The effect of stochastic resonance on Chua's circuit dynamics has been thoroughly investigated, revealing complex phenomena that can be triggered by stochastic perturbations in nonlinear systems [28, 29]. Additionally, Gaussian noise has been employed to simulate the stochastic phenomena in this circuit, with its effective intensity range also being determined [30]. In summary, a comprehensive investigation into the combined effects of impulsive perturbations and stochastic noise on Chua's circuit is of great theoretical importance and provides practical guidance for optimizing real-world systems and designing robust control strategies.

Current control strategies for Chua's circuit primarily focus on improving steady-state performance [31–34], with insufficient attention paid to dynamic performance regulation, particularly the convergence rate (CR). The CR directly determines the system's application in various engineering scenarios, such as signal synchronization in chaotic communications and response speed adjustment in emergency control, making its regulation critically important. Literature [35] provides core research on convergence performance in nonlinear systems. Through in-depth analysis of the relationship between uncertainties and convergence, it clearly reveals the essential challenge of convergence regulation under complex disturbances. This approach offers valuable inspiration, drawing further attention to the coupled impulsive and stochastic disturbances often encountered by Chua's circuit in practice. Consequently, controlling the CR under such composite disturbances becomes a central research objective. As research progresses, some scholars have begun exploring the correlation between system poles and performance metrics, highlighting the importance of interval stability [36–38]. These studies establish a solid theoretical foundation for optimizing control strategies. Building on this groundwork, this paper proposes a fuzzy control scheme with a variable CR for Chua's circuit under simultaneous impulsive and stochastic disturbances. The scheme aims to ensure both steady-state performance and dynamic response quality, enabling the system to achieve stability at a desired CR even under

composite disturbances. The main contributions of this paper are as follows:

(1) A unified stability analysis framework with a variable CR is proposed. Specifically, for Chua's circuit systems under simultaneous impulsive and stochastic disturbances, an interval stability criterion is established based on the generalized pole placement principle and the T-S fuzzy model. This criterion integrates both the stability margin and the dynamic CR, overcoming the limitation of traditional stability theory that merely assesses stability. It thereby enables a quantitative characterization and comprehensive analysis of the CR as a key dynamic performance metric.

(2) A fuzzy controller with actively tunable CR has been designed. Unlike traditional approaches, this work explicitly incorporates the CR as a direct design constraint into the controller synthesis process. This method not only guarantees the mean-square asymptotic stability of the system but also enables active and precise CR regulation, achieving an on-demand design of the system's dynamic performance.

(3) An intelligent algorithm for adjusting the CR has been developed. As an engineering implementation of the theoretical framework, this algorithm dynamically tunes CR parameters according to the system's real-time state. Consequently, it enables intelligent switching of dynamic response modes in Chua's circuit to meet varying application demands.

Notation: $\mathbb{E}[\cdot]$ mathematical expectation operator. $\partial_{min}(\rho)$ denotes the set of impulse time sequences satisfying $\partial_{min}(\rho) := \{\{t_\kappa\}_{\kappa=0}^{\infty} | \inf_\kappa\{t_\kappa - t_{\kappa-1}\} \geq \rho\}$, and $\partial_{max}(\rho)$ satisfying $\partial_{max}(\rho) := \{\{t_\kappa\}_{\kappa=0}^{\infty} | \sup_\kappa\{t_\kappa - t_{\kappa-1}\} \leq \rho\}$. $L_2[0,\infty] := \{x \in R^p | (\int_0^\infty \| x(t) \|^2 dt)^{\frac{1}{2}} < \infty\}$, where $x = (x_1, x_2, \cdots, x_p)^T$. In symmetric block matrices, the symbol $*$ denotes the transpose of the off-diagonal block.

2. Model description and preliminaries

2.1. Chua's circuit system modeling

This section focuses on the modeling of Chua's circuit system. As shown in Figure 1(a), it is a typical chaotic system consisting of an inductor L, a resistor R, two capacitors C_1 and C_2, and a Chua's diode R_2. The circuit is a typical chaotic system. Consider the circuit under impulsive and stochastic disturbances as illustrated in Figure 1(b), while Figure 1(c) depicts the distinctive piecewise-linear voltage-current relationship of R_2.

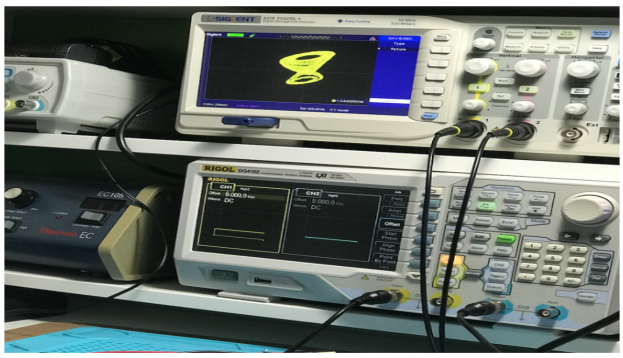

Figure 1(a). Physical realization of Chua's circuit.

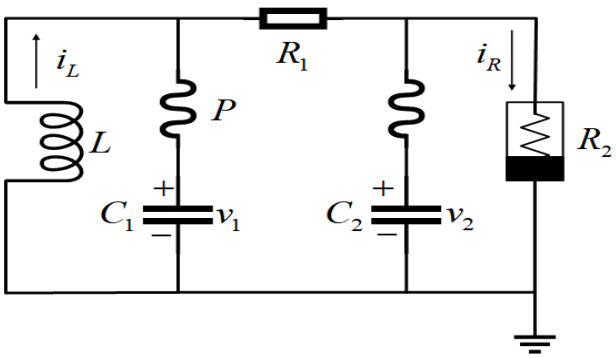

Figure 1(b). Chua's circuit affected by impulses.

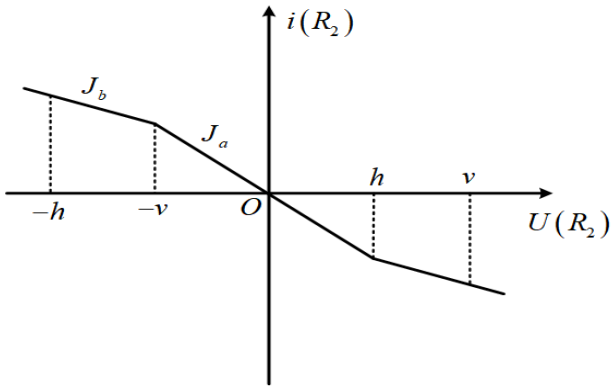

Figure 1(c). The piecewise-linear current-voltage characteristic of the Chua's diode.

The dynamic performance of the Chua's circuit can be described by the following equations:

$$\begin{cases} \dfrac{dv_1}{d\tau} = \dfrac{1}{C_1}(\dfrac{1}{R}(v_2 - v_1) - f(v_1)) + u_1(\tau),\ \tau \neq \tau_\kappa, \\ \dfrac{dv_2}{d\tau} = \dfrac{1}{C_2}(\dfrac{1}{R}(v_1 - v_2 + i) + u_2(\tau),\ \tau \neq \tau_\kappa, \\ \dfrac{di}{d\tau} = -\dfrac{1}{L}v_2 + u_3(\tau),\ \tau \neq \tau_\kappa, \\ v_1(\tau) = (\varsigma_1 + 1)v_1(\tau^-),\ \tau = \tau_\kappa, \\ v_2(\tau) = (\varsigma_2 + 1)v_2(\tau^-),\ \tau = \tau_\kappa, \\ i(\tau) = (\varsigma_i + 1)i(\tau^-),\ \tau = \tau_\kappa, \end{cases} \tag{1}$$

where $f(v_1(\tau)) = J_b v_1 + \frac{1}{2}(J_a - J_b)(|\ v_1 + V\ | - |\ v_1 - V\ |)$. $\{\tau_\kappa\}$ are the impulsive time series, which satisfy $0 \leq \tau_0 < \tau_1 < \tau_2 < \cdots < \tau_\kappa < \cdots$, $\lim\limits_{\kappa \to +\infty} \tau_\kappa = +\infty$. Define $\Delta x(\tau_\kappa) = x(\tau_\kappa^+) - x(\tau_\kappa^-)$, and $x(\tau_\kappa^+) = \lim\limits_{\tau \to \tau_\kappa^+} x(\tau) = x(\tau_\kappa)$, $x(\tau_\kappa^-) = \lim\limits_{\tau \to \tau_\kappa^-} x(\tau)$. Define $x_1 = v_1/V$, $x_2 = v_2/V$, $x_3 = Ri/V$, $t = \tau/RC_2$, $a = RJ_a$, $b = RJ_b$, $x_3 = Ri/V$, $\varpi = \frac{C_2}{C_1}$, and $\varphi = \frac{C_2 R^2}{L}$. (1) is normalized into the dimensionless canonical form:

$$\begin{cases} \dot{x}_1(t) = \varpi(x_2(t) - x_1(t) - f(x_1(t))) + u_1(t),\ t \neq t_\kappa, \\ \dot{x}_2(t) = x_1(t) - x_2(t) + x_3(t) + u_2(t),\ t \neq t_\kappa, \\ \dot{x}_3(t) = -\varphi x_2(t) + u_3(t),\ t \neq t_\kappa, \\ x_1(t) = (\varsigma_1 + 1)x_1(t^-),\ t = t_\kappa, \\ x_2(t) = (\varsigma_2 + 1)x_2(t^-),\ t = t_\kappa, \\ x_3(t) = (\varsigma_i + 1)x_3(t^-),\ t = t_\kappa, \end{cases} \tag{2}$$

where $\dot{x} = dx/dt$, $f(x_1(t)) = bx_1 + \frac{1}{2}(a - b)(|\ x_1 + V\ | - |\ x_1 - V\ |)$, and $f(x_1) \in [-e, e]$ $(e > V > 0)$.

2.2. Chua's circuit model based on T-S fuzzy system

In practical circuit systems, proactive impulsive control actions or external abrupt interference manifest as impulsive effects, while persistent uncertainties such as component thermal noise and parameter fluctuations can be modeled as stochastic disturbances [24]. To capture this, the system is modeled using a T-S fuzzy approach with the following rules:

Rule i: If $\varrho_1(t)$ is z_{i1} and $\varrho_2(t)$ is z_{i2} and, $\cdots$, and $\varrho_p(t)$ is z_{ip}, then,

$$\begin{cases} dx(t) = A_i x(t)dt + B_i u(t)dt + G_i x(t)d\omega(t), \ t \neq t_\kappa, \\ \triangle x(t) = A_{i\kappa} x(t^-), \ t = t_\kappa, \end{cases}$$

where $i = \overline{1, l}$, l represents the number of rules, $z_{ij}(j = \overline{1, p})$ denotes the fuzzy set, $\varrho_j(t)$ is the j-th premise variable, and matrices $A_i \in \mathcal{R}^{n\times n}$, $G_i \in \mathcal{R}^{n\times n}$, and $A_{i\kappa} \in \mathcal{R}^{n\times n}$ are certain system matrices.

Using the singleton fuzzifier, the product inference engine and the center average defuzzifier, system (2) can be written as

$$\begin{cases} dx(t) = \sum\limits_{i=1}^{l} \omega_i(\varrho(t))[A_i x(t) + B_i u(t)]dt + G_i x(t)d\omega(t), \ t \neq t_\kappa, \\ \triangle x(t) = \sum\limits_{i=1}^{l} \omega_i(\varrho(t^-))A_{i\kappa} x(t^-), \ t = t_\kappa, \end{cases} \tag{3}$$

where $\omega_i(\varrho(t)) = \frac{\nu_i(\varrho(t))}{\sum\limits_{i=1}^{l} \nu_i(\varrho(t))}$, $\nu_i(\varrho(t)) = \prod\limits_{j=1}^{p} z_{ij}(\varrho_j(t))$, and $z_{ij}(\varrho_j(t))$ is the membership function grade of premise $\varrho_j(t)$ in z_{ij}. Suppose $\nu_i(\varrho(t)) \geq 0$, then $\omega_i(\varrho(t)) \geq 0$ and $\sum\limits_{i=1}^{l} \omega_i(\varrho(t)) = 1$ hold.

Definition 1. *[39] $\forall x(0) \in \mathcal{R}^n$. System* (3) *is asymptotically mean-square stable (AMSS) if*

$$\lim_{t\to\infty} \mathbb{E}[\|x(t)\|^2] = 0.$$

Definition 2. *[40] Let $\mathcal{L}_{A_i,G_i}$ denote the linear operator associated with system (3) defined by*

$$\mathcal{L}_{A_i,G_i} : X \mapsto A_i X + XA_i^T + G_i X G_i^T \in \mathcal{S}_n,$$

if there exist $\lambda \in \mathbb{C}$ and nonzero $X \in \mathcal{S}_n$ satisfying the spectral equation $\mathcal{L}_{A_i,G_i} X = \lambda X$, where λ is termed an eigenvalue of the operator and X is the corresponding eigenvector. The spectrum $\sigma(\mathcal{L}_{A_i,G_i})$ denotes the set of all such eigenvalues.

Definition 3. *[24] The system (3) achieves asymptotically mean-square stable with a variable convergence rate (AMSSVCR), if there exists $\Re(\sigma(\mathcal{L}_{A_i,G_i})) \subset (-m, -n)$.*

Remark 1. *Through the definition of the system operator $\mathcal{L}_{A_i,G_i}$, the convergence behavior of the system can be characterized. Given that the system is AMSS, its CR changes according to the intervals of the real parts of the eigenvalues.*

Lemma 1. *[41] Consider stochastic differential systems*

$$dx(t) = g_1(t, x(t))dt + g_2(t, x(t))d\omega(t),$$

on $t > 0$ and $x(t_0) = x_0 \in \mathcal{R}^n$. If $V \in C^{2,1}(\mathcal{R}^n \times \mathcal{R}^+; \mathcal{R})$, then $V(x, t)$ represents an Itô process fulfilling the equation below:

$$\begin{aligned} dV(x,t) =& \mathcal{L}Vdt + V_x^T g_2(x,t)d\omega(t) \\ =& [V_t(x,t) + \frac{1}{2} trace[g_2^T(x,t)V_{xx}(x,t)g_2(x,t)] + V_x(x,t)g_1(x,t)]dt \\ &+ V_x^T(x,t)g_2(x,t)d\omega(t). \end{aligned}$$

Lemma 2. *[39] System (2) is said to be AMSS if*

$$A_iP + PA_i^T + G_iPG_i^T < 0,$$

or

$$A_i^TP + PA_i + G_i^TPG_i < 0,$$

where $P > 0$.

3. Main results

3.1. Stability of variable CR

In this section, we discuss the AMSS of variable CR driven by m and n. Setting $u(t) = 0$ in system (3) yields the following system:

$$\begin{cases} dx(t) = \sum_{i=1}^{l} \omega_i(\varrho(t))A_ix(t)dt + G_ix(t)d\omega(t),\ t \neq t_\kappa, \\ \triangle x(t) = \sum_{i=1}^{l} \omega_i(\varrho(t^-))A_{i\kappa}x(t^-),\ t = t_\kappa. \end{cases} \tag{4}$$

Theorem 1. *Let m and n be real numbers with strict hierarchy $m > n \geq 0$, and assume there exists ζ, the existence of a positive definite matrix X and scalar $\xi > 0$ satisfying*

$$\begin{bmatrix} -\xi X & X(A_{i\kappa} + I)^T \\ * & -X \end{bmatrix} < 0, \tag{5}$$

$$\begin{bmatrix} \Upsilon_{1i} & XG_i^T \\ * & -X \end{bmatrix} < 0, \tag{6}$$

$$\begin{bmatrix} \Upsilon_{2i} & XG_i^T \\ * & -X \end{bmatrix} < 0, \tag{7}$$

where

$$\Upsilon_{1i} = \frac{\ln \xi}{\zeta}X + (A_i + nI)X + X(A_i + nI)^T,$$
$$\Upsilon_{2i} = \frac{\ln \xi}{\zeta}X - (A_i + mI)X - X(A_i + mI)^T.$$

Then, system (4) is AMSSVCR on $\partial_{\gamma,\delta}$ driven by m and n. For arbitrary nonnegative scalars γ and δ, let $\partial_{\gamma,\delta}$ indicate that t_κ satisfies

$$\ln \xi\mathcal{N}(t, l) \leq \gamma + (\frac{\ln \xi}{\zeta} - \delta)(t - l),\ t \geq l \geq t_0. \tag{8}$$

Proof. Based on Definition 3, the system achieves AMSSVCR if system (4) is AMSS and satisfies $\Re(\sigma(\mathcal{L}_{A_i,G_i})) \in (-m, \infty)$ and $\Re(\sigma(\mathcal{L}_{A_i,G_i})) \in (-\infty, -n)$. Accordingly, it is analyzed as follows:

$$\begin{cases} dx(t) = \sum_{i=1}^{l} \omega_i(\varrho(t))((A_i + nI)x(t)dt + G_i x(t)d\omega(t)), \ t \neq t_\kappa, \\ \triangle x(t) = \sum_{i=1}^{l} \omega_i(\varrho(t^-))A_{i\kappa}x(t^-), \ t = t_\kappa, \end{cases} \tag{9}$$

and

$$\begin{cases} dx(t) = \sum_{i=1}^{l} \omega_i(\varrho(t))(-(A_i + mI)x(t)dt + G_i x(t)d\omega(t)), \ t \neq t_\kappa, \\ \triangle x(t) = \sum_{i=1}^{l} \omega_i(\varrho(t^-))A_{i\kappa}x(t^-), \ t = t_\kappa. \end{cases} \tag{10}$$

Let $X^{-1} = P$. By performing a congruence transformation on both sides of Eq (6) with the block-diagonal matrix diag $\{P, P\}$, followed by applying Schur's complement lemma, the following transformed inequality is established:

$$\frac{\ln \xi}{\zeta} P + P(nI + A_i) + (nI + A_i)^T P + G_i^T P G_i < 0.$$

For any given $\varepsilon > 0$, one can find a scalar $\varsigma \in (0, \varepsilon)$ satisfying the inequality constraints:

$$\xi' P + P(nI + A_i) + (nI + A_i)^T P + G_i^T P G_i < 0, \tag{11}$$

where $\xi' = \frac{\ln \xi}{\zeta} + \varsigma$.

Similarly, performing a congruence transformation on both sides of Eq (5) with the block-diagonal matrix diag $\{P, P\}$, and then applying Schur's complement lemma leads to

$$(A_{i\kappa} + I)^T P(A_{i\kappa} + I) - \xi P < 0. \tag{12}$$

For system (9), the Lyapunov functional is defined as $V(x(t)) = x^T(t)Px(t)$, leading to the following result:

$$\begin{aligned} V(x(t_\kappa)) &= \sum_{i=1}^{l} \omega_i(\varrho(t^-))x^T(t_\kappa^-)(A_{i\kappa} + I)^T P(A_{i\kappa} + I)x(t_\kappa^-) \\ &\leq \xi \sum_{i=1}^{l} \omega_i(\varrho(t^-))x^T(t_\kappa^-)Px(t_\kappa^-) \\ &\leq \xi V(x(t_\kappa^-)). \end{aligned} \tag{13}$$

Itô's formula yields, for any $t \in [t_\kappa, t_{\kappa+1})$,

$$\begin{aligned} \mathcal{L}V(x(t)) = &\sum_{i=1}^{l} \omega_i(\varrho(t))x^T(t)[P(A_i + nI) + (A_i + nI)^T P]x(t) \\ &+ x^T(t)G_i^T P G_i x(t). \end{aligned} \tag{14}$$

Substituting (11) into (14) gives

$$\mathcal{L}V(x(t)) \leq -\xi' V(x(t)),\ t \in [t_\kappa, t_{\kappa+1}), \tag{15}$$

which leads to the following result:

$$dV(x(t)) \leq \sum_{i=1}^{l} \omega_i(\varrho(t)) 2x^T(t) P G_i(t) x(t) d\omega(t) - \xi' V(x(t)) dt. \tag{16}$$

Applying the stochastic product rule to $e^{\xi' t} V(x(t))$ and substituting Eq (16) yields

$$d(e^{\xi' t} V(x(t))) \leq \sum_{i=1}^{l} \omega_i(\varrho(t)) 2e^{\xi' t} x^T(t) P G_i(t) x(t) d\omega(t). \tag{17}$$

By integrating the preceding expression over $[t_\kappa, t]$ and applying the expectation operator, we obtain the stochastic evolution inequality:

$$\mathbb{E}[V(x(t))] \leq e^{-\xi'(t-t_\kappa)} \mathbb{E}[V(x(t_\kappa))],\ t \in [t_\kappa, t_{\kappa+1}). \tag{18}$$

Substituting (13) into the above equation, we obtain

$$\mathbb{E}[V(x(t))] \leq \xi e^{-\xi'(t-t_\kappa)} \mathbb{E}[V(x(t_\kappa^-))],\ t \in [t_\kappa, t_{\kappa+1}). \tag{19}$$

For $t \in [t_\kappa, t_{\kappa+1})$, integrating (19) yields

$$\begin{aligned} \mathbb{E}[V(x(t))] \leq & \mathbb{E}[\xi^t e^{-\xi'(t-t_0)} V(x(t_0))] \\ \leq & e^\gamma + (\frac{\ln \xi}{\zeta} - \delta)(t - t_0) \mathbb{E}[e^{-\xi'(t-t_0)} V(x(t_0))] \\ \leq & \mathbb{E}[e^\gamma e^{-\varsigma(t-t_0)} V(x(t_0))]. \end{aligned} \tag{20}$$

Invoking the Rayleigh quotient $\lambda_{min}(P)\|x(t)\|^2 \leq V(x) \leq \lambda_{max}(P)\|x(t)\|^2$, we obtain

$$\mathbb{E}[\|x(t)\|^2] \leq \frac{\lambda_{max}(P) e^\gamma}{\lambda_{min}(P)} \mathbb{E}[\xi e^{-\varsigma(t-t_0)} \|x(t_0)\|^2]. \tag{21}$$

This consequently yields the AMSS condition $\lim_{t\to\infty} \mathbb{E}[\|x(t)\|^2] = 0$, which establishes that system (9) is AMSS under the perturbation bounds $\partial_{\gamma,\delta}$. Furthermore, the spectral characterization $\Re(\sigma(\mathcal{L}_{A_i,G_i})) \in (-\infty, -n)$ is derived.

By analogous methodology, the stability criteria (5) and (7) for system (10) can be obtained through parallel derivations, thereby guaranteeing its AMSS property with the following formal characterization:

$$-P(A_i + mI) - (A_i + mI)^T P + G_i^T P G_i < 0. \tag{22}$$

Since $G_i^T P G_i \geq 0$, therefore,

$$-P(A_i + mI) - (A_i + mI)^T P - G_i^T P G_i < 0. \tag{23}$$

By Definition 2, we get $\Re(\sigma(\mathcal{L}_{A_i,G_i})) \in (-m, \infty)$. This completes the proof.

Remark 2. *Under the condition $\xi \geq 1$, the impulsive dynamics manifest as perturbative disturbances. Under this regime, Eq (8) can be reformulated into*

$$\mathcal{N}(t,l) \leq \frac{t-l}{\phi} + \mathcal{N}', \ t_0 \leq l \leq t, \tag{24}$$

where $\phi = \frac{\ln \xi}{\ln \xi/\zeta - \delta}$ and $\mathcal{N}' = \frac{\gamma}{\ln \xi}$. The parameter ϕ specifies the minimum allowable average inter-impulse interval, which effectively excludes the occurrence of unlimited pulses within a limited period of time.

Remark 3. *When the impulse gain satisfies $\xi < 1$, the impulsive control actions exhibit stabilizing properties. Under this condition, Eq (8) can be reformulated as*

$$\mathcal{N}(t,l) \geq \frac{t-l}{\phi} - \mathcal{N}', \ t_0 \leq l \leq t, \tag{25}$$

where $\phi = \frac{\ln(1/\xi)}{\ln(1/\xi)/\zeta + \delta}$, $\mathcal{N}' = \frac{\gamma}{\ln(1/\xi)}$, and where ϕ quantifies the maximum allowable average interval between consecutive stabilizing impulses.

Remark 4. *Theorem 1 establishes a sufficient condition for analyzing the system's stochastic stability and characterizing its CR. Specifically, when the system satisfies the AMSS condition with all eigenvalues confined within the interval $(-m, -n)$, system (4) is guaranteed to maintain AMSS properties while exhibiting distinct exponential mean-square convergence characteristics.*

Remark 5. *The selection of convergence rate parameters m and n (satisfying $m > n \geq 0$) directly determines the dynamic performance. Shifting the interval $(-m, -n)$ leftward accelerates convergence, but their ratio must be properly coordinated to ensure linear matrix inequality (LMI) feasibility. The design of impulse parameters aims to simulate the impulsive dynamics of practical systems: The interval threshold ζ is set according to the impulse frequency density of the simulated system, while the strength constraint ξ is determined based on the nature of the impulses, with $\xi > 1$ for suppressing disturbing impulses and $\xi < 1$ for assisting stabilizing impulses.*

Let $\partial_1^{ave}[\phi, \mathcal{N}']$ and $\partial_2^{ave}[\phi, \mathcal{N}']$ denote the admissible impulsive sequences corresponding to constraints (23) and (24), respectively. This characterization leads to the following fundamental conclusions.

Corollary 1. *Given a scalar $\zeta > 0$, if there exists a matrix X and a scalar $\xi > 0$, satisfying conditions (6)–(8), then system (4) exhibits AMSSVCR under specific impulsive sequences; for all $\mathcal{N}' \geq 0$, when $\xi \geq 1$ with $\phi \geq \zeta$, this stability is achieved over $\partial_1^{ave}[\phi, \mathcal{N}']$, whereas for $\xi < 1$ with $\phi \leq \zeta$, the stability holds over $\partial_2^{ave}[\phi, \mathcal{N}']$.*

3.2. Stabilization of variable CR

Next, we will study the calibration of (3) and design a fuzzy controller to realize the calibration of variable CR driven by m and n.

The design of the controller is given below:

Plant rule i: If $\varrho_1(t)$ is z_{i1} and, $\cdots$, and $\varrho_p(t)$ is z_{ip}, then,

$$u_i(t) = K_i x(t), \ i = 1, 2, \cdots, s, \tag{26}$$

where $K_i \in R^{m\times n}$ represent the matrices yet to be recognized, and the integral controller is

$$u_i(t) = \sum_{i=1}^{l} \omega_i(\varrho(t))K_i x(t). \tag{27}$$

Substituting (27) into system (3), we can obtain

$$\begin{cases} dx(t) = \sum\limits_{i=1}^{l} \omega_i(\varrho(t))[(A_i + B_iK_i)x(t)]dt + G_i x(t)d\omega(t),\ t \neq t_\kappa, \\ \triangle x(t) = \sum\limits_{i=1}^{l} \omega_i(\varrho(t^-))A_{i\kappa}x(t^-),\ t = t_\kappa. \end{cases} \tag{28}$$

Theorem 2. *Let m and n be real numbers with strict hierarchy $m > n \geq 0$, and assume there exists $\zeta > 0$, the existence of a positive definite matrix X, and scalar $\xi > 0$ satisfying*

$$\begin{bmatrix} -\xi X & X(A_{i\kappa} + I)^T \\ * & -X \end{bmatrix} < 0, \tag{29}$$

$$\begin{bmatrix} \Upsilon'_{1i} & XG_i^T \\ * & -X \end{bmatrix} < 0, \tag{30}$$

$$\begin{bmatrix} \Upsilon'_{2i} & XG_i^T \\ * & -X \end{bmatrix} < 0, \tag{31}$$

where

$$\Upsilon'_{1i} = \frac{\ln \xi}{\zeta}X + (A_i + nI)X + X(A_i + nI)^T + B_iY_i + Y_i^T B_i^T,$$
$$\Upsilon'_{2i} = \frac{\ln \xi}{\zeta}X - (A_i + mI)X - X(A_i + mI)^T - B_iY_i - Y_i^T B_i^T.$$

When $\xi \geq 1$, system (28) is AMSSVCR on $\partial_{1-ave}[\phi, \mathcal{N}_0]$ driven by m and n, under the action of the controller (27) with $K_i = Y_iX^{-1}$. Conversely, under the same conditions, when $\xi < 1$, system (28) is AMSSVCR on $\partial_{2-ave}[\phi, \mathcal{N}_0]$ driven by m and n under the action of the controller (27) with $K_i = Y_iX^{-1}$.

Proof. Replace A_i in Theorem 1 with $A_i + B_iK_i$, and let $K_i = Y_iX^{-1}$. The remaining components of the proof share similarities with Theorem 1 and will not be redundantly discussed.

A less conservative criterion ensuring the AMSS of system (28) can be established by relaxing the requirements in Theorem 2, as presented in the following proposition.

Corollary 2. *Let ζ be a positive scalar, and assume the existence of $X > 0$ and a scalar $\xi > 0$, satisfying*

$$\begin{bmatrix} -\xi X & X(A_{i\kappa} + I)^T \\ * & -X \end{bmatrix} < 0, \tag{32}$$

$$\begin{bmatrix} \Upsilon''_i & XG_i^T \\ * & -X \end{bmatrix} < 0, \tag{33}$$

where

$$\Upsilon_i'' = \frac{\ln \xi}{\zeta} X + A_i X + X A_i^T + B_i Y_i + Y_i^T B_i^T.$$

When $\xi \geq 1$, system (28) is AMSS on $\partial_{1-ave}[\phi, \mathcal{N}_0]$ driven by m and n under the action of the controller (27) with $K_i = Y_i X^{-1}$. Conversely, under the same conditions, when $\xi < 1$, system (28) is AMSS on $\partial_{2-ave}[\phi, \mathcal{N}_0]$ driven by m and n under the action of the controller (27) with $K_i = Y_i X^{-1}$.

Remark 6. *Although the controller design in Corollary 2 shares structural similarities with existing stabilization-oriented controllers, its primary limitation lies in the lack of explicit parameter adjustment guidance for modifying the CR. Theorem 2 addresses this practical challenge by establishing an eigenvalue regulation strategy. Through explicit characterization of the pole-performance relationship, systematic CR tuning can be achieved by strategically constraining the closed-loop eigenvalues within prescribed intervals via parameter adaptation.*

3.3. Design of variable CR algorithm

Algorithm 1 The variable CR algorithm for Chua's circuit

Require: $m > 0$ or $n > 0$;
Ensure: Adjusts system convergence rate;
Set L such that $-m < L < -n$;
Use [Theorem2] to solve the fuzzy controller gain matrix K_1;
if The real parts of the eigenvalues are within the interval $(-m, -n)$ **then**
    Proceed to step 4;
else
    Determine appropriate values for m and n;
end if
while m and n do not meet the system convergence requirements **do**
    if The system converges slowly **then**
        Increment m (i.e., $m = m + 1$);
        Increment n (i.e., $n = n + 1$);
    else
        Decrement m (i.e., $m = m - 1$);
        Decrement n (i.e., $n = n - 1$);
    end if
    Use [Theorem2] to solve the fuzzy controller gain matrices $K_2, K_3, \ldots, K_i$;
end while
Use Eq (28) to solve the fuzzy controller $u(t)$;

Remark 7. *The proposed algorithm establishes a systematic framework for the normalized co design of controller parameters m and n. While an arbitrary $0 \leq n < m$ does not ensure the existence of a solution for Theorem 2, the algorithm can be adapted to adjust the values of m and n to resolve Theorem 2. The CR of the system is bounded by setting the values of m and n to obtain the corresponding controllers.*

4. Simulation example

To comprehensively validate the control strategy, this section conducts simulations for two typical impulse scenarios. Disturbing impulses are utilized to simulate external interference for testing the

controller's robustness and dynamic recovery capability, while stabilizing impulses are employed to reflect proactive control, demonstrating their unique performance in on-demand customization of the convergence rate. The results show the effectiveness of the proposed method.

Example 1. Consider the Chua's circuit equations after parametric transformation:

$$\begin{cases} \dot{x_1} = \varpi(x_2(t) - x_1(t) - f(x_1(t))) + b_1u_1(t), \\ \dot{x_2} = x_1(t) - x_2(t) + x_3(t) + b_2u_2(t), \\ \dot{x_3} = -\varphi x_2(t) + b_3u_3(t), \end{cases} \tag{34}$$

employing parameters $\varpi = 9.38$, $\varphi = 16.25$, $a = -1.24$, $b = -0.68$, and $V = 1$. The chaotic system was initialized with state variables $(x_1, x_2, x_3) = (1.6, -0.3, -1.2)$. Figure 2(a) characterizes the resultant attractor topology under uncontrolled conditions ($u = 0$), revealing the intrinsic nonlinear dynamics of the open-loop system.

Meanwhile, Figure 2(b)–(d) delineates the evolutionary trajectories of system states, revealing inherent instabilities within the system dynamics.

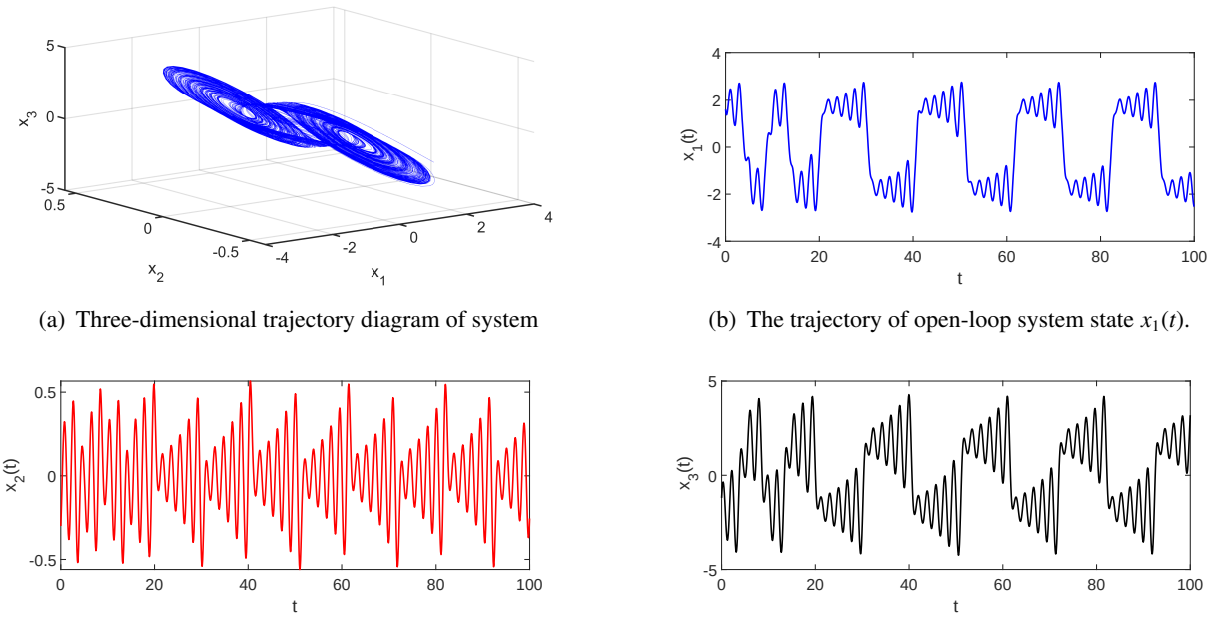

(a) Three-dimensional trajectory diagram of system

(b) The trajectory of open-loop system state $x_1(t)$.

(c) The trajectory of open-loop system state $x_2(t)$.

(d) The trajectory of open-loop system state $x_3(t)$.

Figure 2. The state response of uncontrolled systems.

The membership functions are designed in close alignment with the nonlinear physical mechanism of Chua's circuit.

The capacitor voltage $x_1(t)$, which directly governs the chaotic dynamics, is chosen as the premise variable $\varrho(t)$. The membership functions are constructed directly from the characteristic function of the nonlinear resistor, expressed as $\omega_1(\varrho(t)) = \frac{1}{2}(1-\psi(x_1(t))/h)$ and $\omega_2(\varrho(t)) = \frac{1}{2}(1+\psi(x_1(t))/h)$, where $h = 1.8$. This value is determined based on the actual amplitude range of $x_1(t)$ during chaotic oscillations, ensuring the validity of the membership functions across the entire operating range. The auxiliary function $\psi(x_1(t))$, which accurately captures the piecewise linear nature of the nonlinear resistor, is

defined as:

$$\psi(x_1(t)) = \begin{cases} f(x_1)/x_1, \ x_1 \neq 0, \\ J_a, \ x_1 = 0. \end{cases}$$

The dynamical system under investigation admits an equivalent mathematical representation formulated by the following:

Plant Rule 1: If $\varrho(t)$ is about M_1, then,

$$dx(t) = (A_1 x(t) + B_1 u(t))dt + G_1 x(t) d\omega(t),$$

Plant Rule 2: If $\varrho(t)$ is about M_2, then,

$$dx(t) = (A_2 x(t) + B_2 u(t))dt + G_2 x(t) d\omega(t),$$

where

$$A_1 = \begin{bmatrix} \varpi(h-1) & \varpi & 0 \\ 1 & -1 & 1 \\ 0 & -\varphi & 0 \end{bmatrix}, \quad A_2 = \begin{bmatrix} -\varpi(h+1) & \varpi & 0 \\ 1 & -1 & 1 \\ 0 & -\varphi & 0 \end{bmatrix},$$

$$B_1 = B_2 = I_{3\times 3}, \quad G_1 = G_2 = diag\{0.1 \ 0.1 \ 0.1\}.$$

The impulsive state jump dynamics in the circuit are governed by

$$\Delta x(t) = \begin{bmatrix} 0.5 & 0 & 0 \\ 0 & 0.5 & 0 \\ 0 & 0 & 0.5 \end{bmatrix} x(t^-), \ t = t_\kappa.$$

Following Corollary 2, setting impulse parameters $\xi = 3.2$, $\zeta = 0.2$ in Matlab gives

$$K_1 = \begin{bmatrix} -12.0194 & -5.1900 & 0.0000 \\ -5.1900 & -3.5194 & 7.6250 \\ -0.0000 & 7.6250 & -4.5194 \end{bmatrix}, \quad K_2 = \begin{bmatrix} 21.7446 & -5.1900 & 0.0000 \\ -5.1900 & -3.5194 & 7.8900 \\ -0.0000 & 7.8900 & -4.5194 \end{bmatrix}.$$

The efficacy of the nonlinear control strategy is demonstrated through implementation of the proposed controller (34) in the original dynamical system. As evidenced by the state trajectories in Figure 3, the controlled system exhibits asymptotic convergence to equilibrium beyond $t = 2$ s with all states maintaining bounded operation.

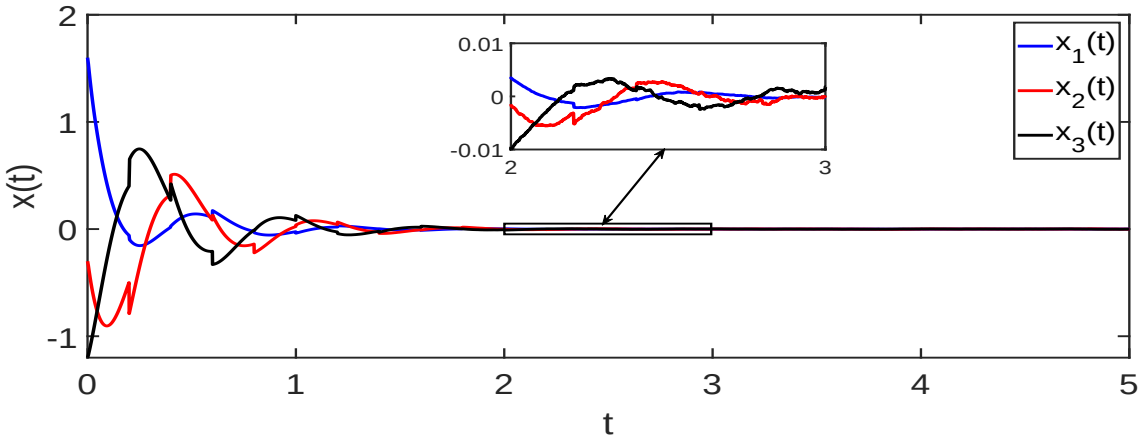

Figure 3. State trajectories under Corollary 2.

Following Theorem 2 with prescribed interval constraints $(-m, -n) = (-3.5, -1.5)$, the corresponding LMIs are formulated and solved to obtain the stabilizing feedback gain matrices:

$$K_1 = \begin{bmatrix} -10.0000 & -5.1900 & 0.0000 \\ -5.1900 & -1.5000 & 7.6250 \\ -0.0000 & 7.6250 & -2.5000 \end{bmatrix}, \quad K_2 = \begin{bmatrix} 23.7640 & -5.1900 & 0.0000 \\ -5.1900 & -1.5000 & 7.8900 \\ -0.0000 & 7.8900 & -2.5000 \end{bmatrix}.$$

The system demonstrates delayed convergence characteristics as evidenced in Figure 4, where all state variables satisfy $|\, x_i(t)\, | < 0.01$ $(i = 1, 2, 3)$ for $t > 10$ s.

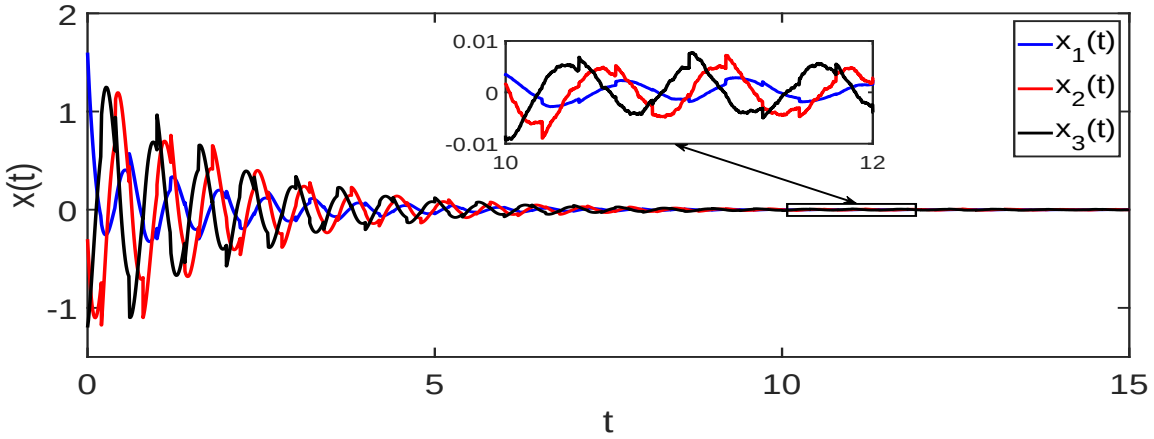

Figure 4. State trajectories in the interval $(-3.5, -1.5)$.

Comparative analysis reveals that prescribing the eigenvalue cluster within the accelerated convergence region $(-8.5, -6.5)$ through Theorem 2's LMI framework significantly improves transient dynamics. The synthesized control gains are as follows:

$$K_1 = \begin{bmatrix} -15.0000 & -5.1900 & -0.0000 \\ -5.1900 & -6.5000 & 7.6250 \\ -0.0000 & 7.6250 & -7.5000 \end{bmatrix}, \quad K_2 = \begin{bmatrix} 18.7640 & -5.1900 & 0.0000 \\ -5.1900 & -6.5000 & 7.8900 \\ 0.0000 & 7.8900 & -7.5000 \end{bmatrix}.$$

Induce rapid stabilization as demonstrated in Figure 5, with all system states achieving convergence within $t > 0.9$ s.

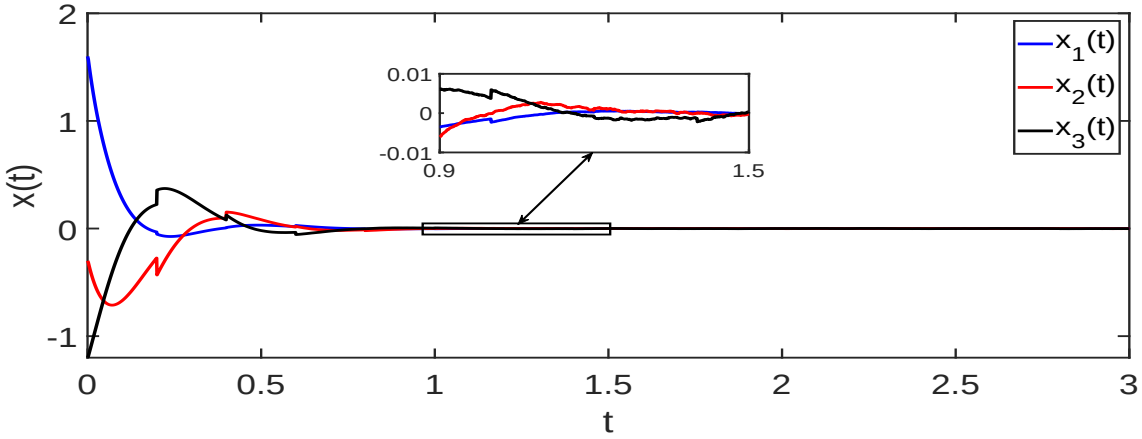

Figure 5. State trajectories in the interval $(-8.5, -6.5)$.

Remark 8. *As demonstrated in Figures 4 and 5, the proposed eigenvalue interval adjustment method enables systematic control of CR through dynamic pole configuration. This tunable mechanism offers significant implementation advantages for Chua's circuit-based systems, particularly in achieving adaptable transient responses and enhanced signal processing capacity through controlled attractor manipulation.*

To compare the convergence rates of different fuzzy control schemes under impulsive disturbances, refer to Table 1.

Table 1. Convergence time of different fuzzy control strategies under impulsive disturbances.

Methods	Traditional method	This paper (fast)	This paper (slow)
Parameters		$(-8.5, -6.5)$	$(-3.5, -1.5)$
Time t at $\|x(t)\|$=0.01	2 s	0.9 s	10 s

As can be seen from Table 1, in the presence of impulsive disturbances, the conventional fuzzy controller requires approximately 2 s to drive the system state to the steady-state interval (± 0.01). In contrast, the convergence time is significantly reduced to 0.9 s with the controller developed in this work. These results convincingly demonstrate that the proposed scheme possesses superior dynamic recovery capability and enhanced robustness when subjected to abrupt external disturbances, thereby effectively improving the system's performance and disturbance rejection.

Example 2. This subsection discusses the Chua's circuit under the influence of a calming pulse. Consider system (34), where the pulse is changed to a pulse of the following form:

$$\Delta x(t) = \begin{bmatrix} -0.4 & 0 & 0 \\ 0 & -0.4 & 0 \\ 0 & 0 & -0.4 \end{bmatrix} x(t^{-}),\ t = t_{\kappa},$$

employing parameters $\varpi = 9.38$, $\varphi = 16.25$, $a = -1.24$, $b = -0.68$, and $V = 1$. Set the initial conditions of the system as $x_1 = 1.6$, $x_2 = -0.3$, and $x_3 = -1.2$.

From Corollary 2, setting impulse parameters $\xi = 0.85$ and $\zeta = 0.8$ in Matlab gives

$$K_1 = \begin{bmatrix} -8.0059 & -5.1900 & 0.0000 \\ -5.1900 & 0.4941 & 7.6250 \\ 0.0000 & 7.6250 & -0.5059 \end{bmatrix},\quad K_2 = \begin{bmatrix} 25.7581 & -5.1900 & -0.0000 \\ -5.1900 & 0.4941 & 7.8900 \\ -0.0000 & 7.8900 & -0.5059 \end{bmatrix}.$$

The state stabilization process is quantitatively captured in Figure 6, revealing equilibrium attainment with $t > 3.2$ s.

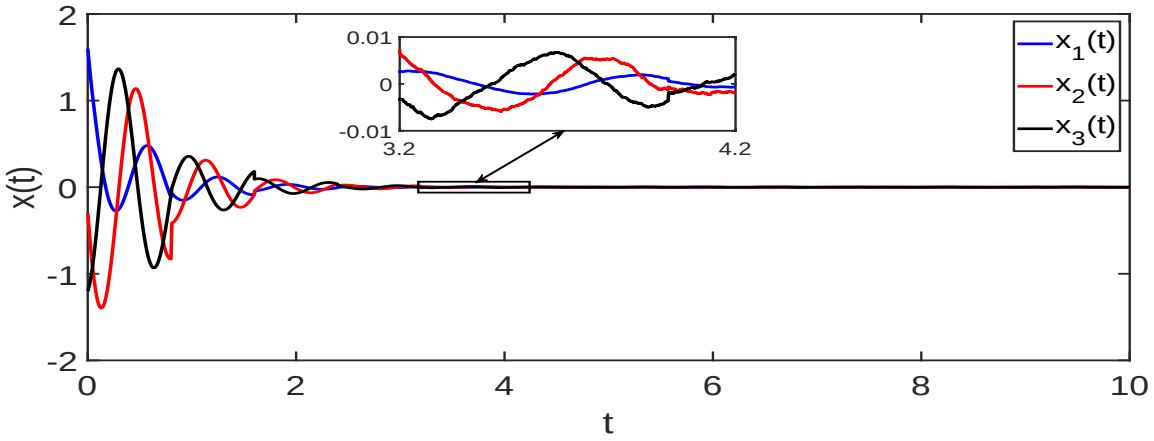

Figure 6. State trajectories under Corollary 2.

Following Theorem 2 with constraint parameters $(-m, -n) = (-0.3, -0.1)$, the LMI solutions produce the following control gains:

$$K_1 = \begin{bmatrix} -7.7000 & -5.1900 & 0.0000 \\ -5.1900 & 0.8000 & 7.6250 \\ -0.0000 & 7.6250 & -0.2000 \end{bmatrix}, \quad K_2 = \begin{bmatrix} 26.0640 & -5.1900 & 0.0000 \\ -5.1900 & 0.8000 & 7.8900 \\ -0.0000 & 7.8900 & -0.2000 \end{bmatrix}.$$

The resultant closed-loop dynamics exhibit delayed stabilization (settling time $t > 3.9\ s$), as shown in Figure 7, requiring 3.9 seconds to achieve $| x_i(t) | < 0.01 (i = 1, 2, 3)$.

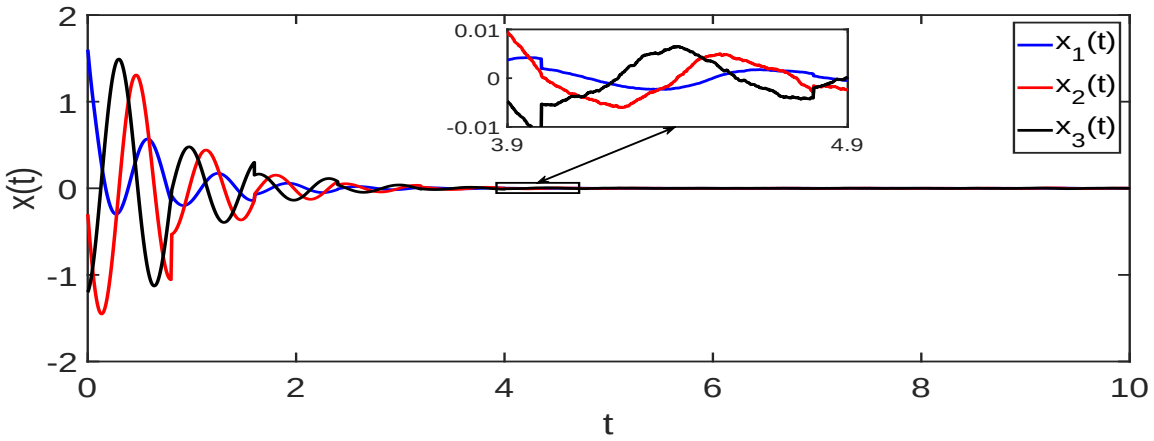

Figure 7. State trajectories in the interval $(-0.3, -0.1)$.

Adopting accelerated convergence parameters $(-3.5, -1.5)$ in Theorem 2, the LMI solutions generate optimized gains as follows:

$$K_1 = \begin{bmatrix} -10.0000 & -5.1900 & -0.0000 \\ -5.1900 & -1.5000 & 7.6250 \\ -0.0000 & 7.6250 & -2.5000 \end{bmatrix}, \quad K_2 = \begin{bmatrix} 23.7640 & -5.1900 & -0.0000 \\ -5.1900 & -1.5000 & 7.8900 \\ -0.0000 & 7.8900 & -2.5000 \end{bmatrix}.$$

Figure 8 depicts the closed-loop system's transient response, showing all state variables converging to equilibrium within approximately $t > 1.5\ s$.

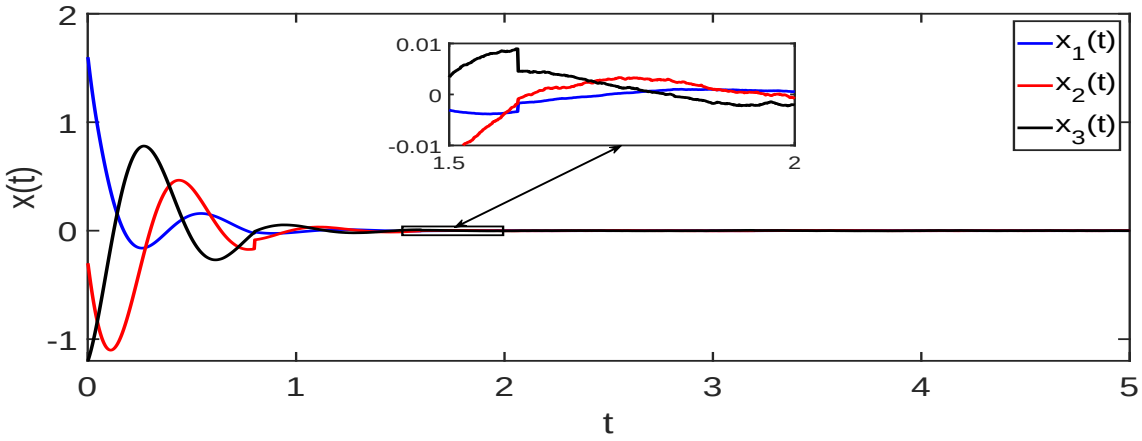

Figure 8. State trajectories in the interval $(-3.5, -1.5)$.

Remark 9. *By flexibly adjusting the convergence rate of Chua's circuit under different impulsive influences, the proposed strategy enables the system to demonstrate high efficiency in fast-response scenarios (e.g., real-time communication and emergency control) while also functioning effectively in scenarios requiring slow dynamic responses (e.g., cryptographic security and bionics). The engineering implementation of this strategy features low barriers, as its core algorithm has manageable computational complexity and can be embedded into low-cost hardware for real-time operation without requiring additional specialized equipment. Hardware costs remain compatible with existing systems. This combination of high feasibility and on-demand programmability provides key technical support for customized applications of chaotic systems in fields such as communications, control, security, and healthcare, significantly enhancing the adaptability of the system from theoretical design to engineering implementation.*

To compare the convergence rates of different fuzzy control schemes under stabilizing impulses, refer to Table 2.

Table 2. Convergence time of different fuzzy control strategies under stabilizing impulses.

Methods	Traditional method	This paper (fast)	This paper (slow)
Parameters		$(-3.5, -1.5)$	$(-0.3, -0.1)$
Time t at $\|x(t)\|$=0.01	3.2 s	1.5 s	3.9 s

As can be seen from Table 2, in control scenarios that use stabilizing impulses, it works together with the impulses to achieve faster convergence (1.5 s) than traditional methods (3.2 s). Moreover, the convergence process can also be adjusted as needed, for example, to a slower 3.9 s duration. This wide range of control, from fast stabilization to slow operation, overcomes the limited performance of conventional controllers. It allows the system's dynamic response to be intelligently shaped for both fast and slow needs.

5. Conclusions

This paper systematically addresses the intelligent control of dynamic CR in Chua's circuits subject to impulsive and stochastic disturbances. First, a unified analytical framework capable of

simultaneously quantifying stability margin and CR is established by integrating generalized pole placement with T-S fuzzy modeling. Subsequently, based on this framework, a fuzzy controller is designed to actively regulate the CR, enabling precise shaping of the system's dynamic performance. Finally, an intelligent adjustment algorithm is developed, successfully achieving online dynamic optimization of the CR. Simulations validate the effectiveness of the proposed approach in enhancing system response performance. Future work will focus on the engineering transformation of the proposed control strategy, including in-depth analysis and optimization of its hardware implementation cost, computational complexity, and real-time processing capability. Meanwhile, the established analytical framework exhibits strong generality and will be extended to other nonlinear circuit systems as well as broader application scenarios such as distributed coordination control in multi-agent systems.

Author contributions

Yining Zhang: Conceptualization, formal analysis, writing-original draft; Xinran Li: Software, methodology, writing-review & editing; Tinglin Zhang: Formal analysis, writing-review & editing; Huasheng Zhang: Validation, visualization. All authors have approved the final manuscript for publication.

Use of Generative-AI tools declaration

The authors declare they have not used Artificial Intelligence (AI) tools in the creation of this article.

Acknowledgments

This work was supported by the Shandong Provincial Natural Science Foundation under Grant ZR2022MF293 and Grant ZR2021JQ23.

Conflict of interest

The authors declare that there are no conflicts of interest.

References

1. W. Zuo, Y. Zhang, J. Song, Y. Zhu, Z. Zhang, Bursting oscillations induced by the variable discontinuous boundary in Chua's circuit, *IEEE Trans. Circuits Syst. I: Reg Papers,* **72** (2025), 2768–2777. https://doi.org/10.1109/TCSI.2025.3553484
2. F. A. Miranda-Villatoro, F. Castaños, A. Franci, Equivalence of linear complementarity problems: theory and application to nonsmooth bifurcations, *IEEE Trans. Autom. Control,* **69** (2024), 4570–4582. https://doi.org/10.1109/TAC.2023.3338981
3. M. Shen, C. Wang, Q. G. Wang, Y. Sun, G. Zong, Synchronization of fractional reaction-diffusion complex networks with unknown couplings, *IEEE Trans. Netw. Sci. Eng.,* **11** (2024), 4503–4512. https://doi.org/10.1109/TNSE.2024.3432997

4. O. Kahouli, I. Zouak, M. A. Hammad, A. Ouannas, M. Ayari, On incommensurate chaotic fractional discrete model of a computer virus: Stabilization and synchronization, *AIMS Math.,* **10** (2025), 19940–19957. https://doi.org/10.3934/math.2025890
5. W. Xue, Y. Zhang, Q. Xu, H. Wu, M. Chen, Initial-condition-controlled synchronization behaviors in inductively coupled memristive Chua's circuits, *Nonlinear Dyn.,* **112** (2024), 10417–10432. https://doi.org/10.1007/s11071-024-09587-8
6. S. Fu, L. Li, J. Feng, Strategy optimization of controlled evolutionary games on a two-layer coupled network using Lebesgue sampling, *Nonlinear Anal-hybri.,* **56** (2025), 101570. https://doi.org/10.1016/j.nahs.2024.101570
7. I. M. Kopp, I. Samuilik, Chaotic dynamics in Sprott's memristive artificial neural network: dynamic analysis, circuit implementation and synchronization, *AIMS Math.,* **10** (2025), 19240–19266. https://doi.org/10.3934/math.2025860
8. W. Chen, W. Xu, W. Zheng, Sliding-mode-based impulsive control for a class of time-delay systems with input disturbance, *Automatica,* **164** (2024), 111633. https://doi.org/10.1016/j.automatica.2024.111633
9. T. Takagi, M. Sugeno, Fuzzy identification of systems and its applications to modeling and control, *IEEE Trans. Syst. Man Cybern.,* **15** (1985), 116–132. https://doi.org/10.1109/TSMC.1985.6313399
10. Z. Hu, X. Mu, J. Mu, Finite-time impulsive control for stochastic T-S fuzzy systems: A waiting-time-based event-triggered method, *Fuzzy Sets Syst.,* **464** (2023), 108428. https://doi.org/10.1016/j.fss.2022.10.020
11. S. Wang, J. Xia, X. Wang, W. Yang, L. Wang, Adaptive neural networks control for MIMO nonlinear systems with unmeasured states and unmodeled dynamics, *Appl. Math. Comput.,* **408** (2021), 126369. https://doi.org/10.1016/j.amc.2021.126369
12. Y. Niu, K. Shi, X. Cai, S. Wen, Adaptive smooth sampled-data control for synchronization of T-S fuzzy reaction-diffusion neural networks with actuator saturation, *AIMS Math.,* **10** (2025), 1142–1161. https://doi.org/10.3934/math.2025054
13. L. Zhang, Z. Li, Y. Li, J. Dong, State and fault interval estimation for discrete-time takagi-sugeno fuzzy systems via intermediate observer base on zonotopic analysis, *IEEE Trans. Fuzzy Syst.,* **32** (2024), 6588–6593. https://doi.org/10.1109/TFUZZ.2024.3459642
14. L. Deng, X. Cao, J. Zhao, One-bit function perturbation impact on robust set stability of boolean networks with disturbances, *Mathematics,* **12** (2024), 2227–7390. https://doi.org/10.3390/math12142258
15. G. Li, C. Peng, Z. Cao, Finite-time bounded asynchronous sliding-mode control for T-S fuzzy time-delay systems via event-triggered scheme, *Fuzzy Sets Syst.,* **514** (2025), 109400. https://doi.org/10.1016/j.fss.2025.109400
16. Y. Liu, S. Zhao, J. Lu, A new fuzzy impulsive control of chaotic systems based on T-S fuzzy model, *IEEE Trans. Fuzzy Syst.,* **19** (2010), 393–398. https://doi.org/10.1109/TFUZZ.2010.2090162

17. C. Liang, M. Ge, Z. Liu, X. Zhan, J. Park, Predefined-time stabilization of T-S fuzzy systems: A novel integral sliding mode-based approach, *IEEE Trans. Fuzzy Syst.,* **30** (2022), 4423–4433. https://doi.org/10.1109/TFUZZ.2022.3152834

18. H. Zhou, J. Zhou, Fixed-time synchronization of quaternion-valued memristive neural networks with time-varying delays and impulsive effect, *AIMS Math.,* **10** (2025), 24093–24114. https://doi.org/10.3934/math.20251069

19. M. Shen, C. Wang, Q. G. Wang, H. Yan, G. Zong, Z. H. Zhu, Fault-tolerant synchronization control of switched complex networks by a proportional-integral intermediate observer approach, *IEEE Trans. Cybern.,* **55** (2025), 4689–4698. https://doi.org/10.1109/TCYB.2025.3591393

20. M. Cheng, J. Zhao, X. Xie, Z. Sun, A novel finite-time stability criteria and controller design for nonlinear impulsive systems, *Appl. Math. Comput.,* **479** (2024), 128876. https://doi.org/10.1016/j.amc.2024.128876

21. G. Liu, Y. Li, X. Yang, Existence and multiplicity of rotating periodic solutions for Hamiltonian systems with a general twist condition, *J. Differ. Equations,* **369** (2023), 229–252. https://doi.org/10.1016/j.jde.2023.06.001

22. X. Liu, Y. M. Zeng, Analytic and numerical stability of delay differential equations with variable impulses, *Appl. Math. Comput.,* **358** (2019), 293–304. https://doi.org/10.1016/j.amc.2019.04.051

23. M. Zhang, Q. Zhu, Stabilization of unstable impulsive systems via stochastic discrete-time feedback control with Levy noise, *Nonlinear Anal.-Hybri.,* **56** (2025), 101585. https://doi.org/10.1016/j.nahs.2025.101585

24. X. Wang, H. Zhang, Intelligent control of convergence rate of impulsive dynamic systems affected by nonlinear disturbances under stabilizing impulses and its application in Chua's circuit, *Chaos Soliton. Fract.,* **169** (2023), 113289. https://doi.org/10.1016/j.chaos.2023.113289

25. C. Zhu, L. He, K. Zhang, Optimal timing fault tolerant control for switched stochastic systems with switched drift fault, *Mathematics,* **10** (2022), 1880. https://doi.org/10.3390/math10111880

26. V. Anishchenko, M. Safonova, L. Chua, Stochastic resonance in Chua's circuit, *Int. J. Bifurcat Chaos*, 1992. https://doi.org/10.1142/9789812798855-0011

27. G. Chen, C. Fan, J. Sun, J. Xia, Mean square exponential stability analysis for Itô stochastic systems with aperiodic sampling and multiple time-delays, *IEEE Trans. Autom. Control,* **67** (2022), 2473–2480. https://doi.org/10.1109/TAC.2021.3074848

28. G. Zhuang, J. Xia, J. Feng, Y. Wang, G. Chen, Dynamic compensator design and H_∞ admissibilization for delayed singular jump systems via Moore-Penrose generalized inversion technique, *Nonlinear Anal.-Hybri.,* **49** (2023), 101361. https://doi.org/10.1016/j.nahs.2023.101361

29. M. Shen, X. Wang, J. H. Park, Y. Yi, W. W. Che, Extended disturbance-observer-based data-driven control of networked nonlinear systems with event-triggered output, *IEEE Trans. Syst. Man Cybern.: Syst.,* **53** (2023), 3129–3140. https://doi.org/10.1109/TSMC.2022.3222491

30. F. Prebianca, H. A. Albuquerque, M. W. Beims, Describing intrinsic noise in Chua's circuit, *Phys. Lett. A,* **382** (2018), 2420–2423. https://doi.org/10.1016/j.physleta.2018.05.054

31. G. Chen, J. Xia, J. H. Park, H. Shen, G. Zhuang, Robust sampled-data control for switched complex dynamical networks with actuators saturation, *IEEE Trans. Cybern.,* **52** (2022), 10909–10923. https://doi.org/10.1109/TCYB.2021.3069813
32. Z. Wang, D. Xu, Z. Li, A general configuration for nonlinear circuit employing current-controlled nonlinearity: Application in Chua's circuit, *Chaos Soliton. Fract.,* **177** (2023), 114233. https://doi.org/10.1016/j.chaos.2023.114233
33. J. Zhao, Y. Yuan, Z. Sun, X. Xie, Applications to the dynamics of the suspension system of fast finite time stability in probability of p-norm stochastic nonlinear systems, *Appl. Math. Comput.,* **457** (2023), 128221. https://doi.org/10.1016/j.amc.2023.128221
34. X. Liu, M. Zhang, Z. W. Yang, Numerical threshold stability of a nonlinear age-structured reaction diffusion heroin transmission model, *Appl. Numer. Math.,* **204** (2024), 291–311. https://doi.org/10.1016/j.apnum.2024.06.016
35. S. Gu, C. Qian, N. Zhang, Finite-time integral control for a class of nonlinear planar systems with non-vanishing uncertainties, *Automatica,* **136** (2022), 110016. https://doi.org/10.1016/j.automatica.2021.110016
36. T. Zhang, H. Zhang, X. Xie, Region stability/stabilization and H_∞ control for discrete-time impulsive takagi-sugeno fuzzy systems, *IEEE Trans. Fuzzy Syst.,* **32** (2024), 3410–3419. https://doi.org/10.1109/TFUZZ.2024.3372936
37. G. Zhuang, J. Xia, J. Feng, B. Zhang, J. Lu, Z. Wang, Admissibility analysis and stabilization for neutral descriptor hybrid systems with time-varying delays, *Nonlinear Anal.-Hybri.,* **33** (2019), 311–321. https://doi.org/10.1016/j.nahs.2019.03.009
38. L. Xia, J. Wang, S. Fu, Control design to minimize the number of bankrupt players for networked evolutionary games with bankruptcy mechanism, *AIMS Math.,* **9** (2024), 35702–35720. https://doi.org/10.3934/math.20241694
39. Y. Deng, H. Zhang, J. Xia, H_∞ control with convergence rate constraint for time-varying delay switched systems, *IEEE Trans. Syst. Man Cybern: Syst.,* **53** (2023), 7354–7363. https://doi.org/10.1109/TSMC.2023.3298813
40. W. Zhang, L. Xie, B. Chen, *Stochastic H_2/H_∞ control-a nash game approach*, CRC Press, 2017. https://doi.org/10.1201/9781315117706
41. W. Chen, J. Wang, Y. Tang, X. Lu, Robust H_∞ control of uncertain linear impulsive stochastic systems, *Int. J. Robust Nonlinear Control,* **18** (2008), 1348–1371. https://doi.org/10.1002/rnc.1286

AIMS Press